THE JOURNAL OF PHYSICAL CHEMISTRY B

Article

pubs.acs.org/JPCB

Assessment of DFT for Computing Sum Frequency Generation Spectra of an Epoxydiol and a Deuterated Isotopologue at Fused Silica/Vapor Interfaces

Hilary M. Chase,[†] Benjamin Rudshteyn,[‡] Brian T. Psciuk,[‡] Mary Alice Upshur,[†] Benjamin F. Strick,[†] Regan J. Thomson,[†] Victor S. Batista,*[,‡] and Franz M. Geiger*[,†]

[†]Department of Chemistry, Northwestern University, Evanston, Illinois 60208, United States

[‡]Department of Chemistry, Yale University, New Haven, Connecticut 06520, United States

Supporting Information

ABSTRACT: We assess the capabilities of eight popular density functional theory (DFT) functionals, in combination with several basis sets, as applied to calculations of vibrational sum frequency generation (SFG) spectra of the atmospherically relevant isoprene oxidation product *trans*-β-isoprene epoxydiol (IEPOX) and one of its deuterated isotopologues at the fused silica/vapor interface. We use sum of squared differences (SSD) and total absolute error (TAE) calculations to estimate the performance of each functional/basis set combination in producing SFG spectra that match experimentally obtained spectra from *trans*-β-IEPOX and one of its isotopologues. Our joined SSD/TAE analysis shows that while the twist angle of the methyl C_{3v} symmetry axis of *trans*-β-IEPOX relative to the surface is sensitive to the choice of DFT functional, the calculated tilt angle relative to the surface normal is largely independent of the functional and basis set. Moreover, we report that hybrid functionals such as B3LYP, ωB97X-D, PBE0, and B97-1 in combination with a modest basis set, such as 6-311G(d,p), provides good agreement with experimental data and much better performance than pure functionals such as PBE and BP86. However, improving the quality of the basis set only improves agreement with experimental data for calculations based on pure functionals. A conformational analysis, based on comparisons of calculated and experimental SFG spectra, suggests that *trans*-β-IEPOX points all of its oxygen atoms toward the silica/vapor interface.

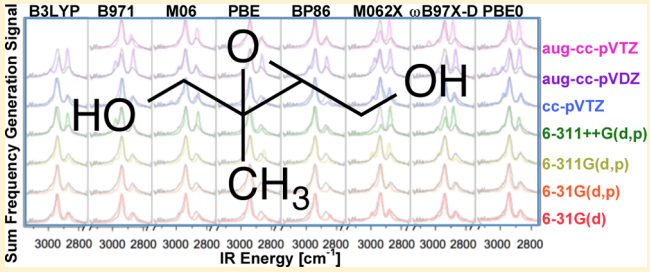

1. INTRODUCTION

Determining molecular structure, orientation, and ordering at interfaces is important for many processes in areas of science and engineering.[1−18] While sum frequency generation (SFG) spectroscopy has provided great molecular insight into the molecular orientation and structure of hydrocarbons or long-chain surfactants at interfaces,[19−27] the interpretation of SFG spectra of strained, oxygenated species, many of which are important in combustion chemistry, catalysis, and atmospheric aerosol science,[8,28−34] is much less straightforward. This difficulty is especially apparent in the C−H stretching region, where overtones, combination bands, and Fermi resonances can make it challenging to reliably assign the observed vibrational features.

One approach to address this difficulty is to pair experimental SFG spectroscopy with the simulation of SFG spectra using ab initio methods such as density functional theory (DFT). While this approach has been successful for understanding molecular structure at interfaces,[3,4,35−41] a comprehensive survey of functionals and basis sets for computing SFG spectra has not yet been carried out in the C−H stretching region, although this has been done for infrared and Raman spectroscopy.[42−49] Two studies assess the appropriateness of various DFT methods and basis sets for computing SFG spectra, but one of them assesses the SFG response from localized vibrational modes of just a single methyl (CH_3) group, rather than multiple vibrations throughout an entire molecule,[50] and the other only addresses a NO stretching mode.[51] These approaches may not necessarily be applicable to molecules containing multiple carbon atoms, as C−H stretching modes may be anharmonic in nature[52−54] and are often delocalized throughout multiple C−H groups in an organic molecule.[55] An assessment of functionals and basis sets for SFG spectroscopic simulations would represent an important step toward the reliable prediction of SFG spectra of strained, oxygenated species, including those that may be too transient to measure spectroscopically or difficult to synthesize.

The computation of SFG signal intensities is not a straightforward task even when the molecular orientation is known, given their dependence on the molecular hyper-

Special Issue: Bruce C. Garrett Festschrift

Received: October 6, 2015
Revised: November 12, 2015

DOI: 10.1021/acs.jpcb.5b09769
J. Phys. Chem. B XXXX, XXX, XXX−XXX

polarizability and therefore the dipole and polarizability derivatives with respect to each normal mode. Given that these values depend on which functional and basis set combination is used,[43,47,56−58] it is important to determine how the computation of SFG spectra depends on the choice of functional and basis set.

The present work aims to do so for a number of popular DFT functionals and basis sets applied to computing the SFG spectrum of *trans*-β-isoprene epoxydiol[13,59−64] (*trans*-β-IEPOX) (Figure 1A), a strained, five-carbon-, three-oxygen-atom-containing oxygenation product important in tropospheric isoprene chemistry.[55] We recently reported that the methyl C_{3v} symmetry axis of this molecule is tilted approximately 70−80° away from the surface normal of a fused silica optical window (see Figure S9 in the Supporting Information) and that the SFG spectrum is largely due to nonlocal normal modes. The DFT-based assignments given in our earlier work[55] show that the one peak that dominates the ssp-polarized SFG spectrum is produced by a nonlocal group oscillator involving largely the methyl symmetric stretch, with minor contributions from the asymmetric stretch of the methylene group adjacent to the carbon bearing the methine hydrogen and the methine stretches. We also compared our experimental and computed SFG spectra to those obtained from isotopologue d_2-*trans*-β-IEPOX (Figure 1B) to provide a measure of reliability for the computed spectra, which turned out to be reasonable.

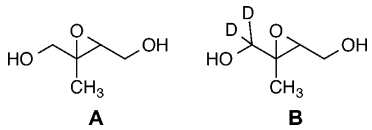

Figure 1. Structures of *trans*-β-IEPOX (A) and d_2-*trans*-β-IEPOX (B).

As mentioned in our earlier work,[55] the DFT-based SFG spectra for the unlabeled and the d_2-deuterated version agree well with the experimental spectra, but only the B3LYP hybrid functional and the 6-311G(d,p) basis set were used. Here, we explore other functional/basis set combinations by computing the spectral sum of squared differences (SSD) between the experimental and simulated SFG spectra using scaled harmonic frequencies. We complement the SSD values with a quantification of differences in computed versus experimentally observed vibrational mode frequencies, as well as differences in computed versus experimentally observed SFG signal intensities so as to provide a benchmark for identifying which model chemistry will produce the best-matching SFG spectrum of the epoxide under investigation.

2. SFG THEORY

The theoretical basis behind SFG has been described elsewhere in previous work.[27,65−70] Briefly, the intensity of the sum frequency signal is given by

$$I_{\mathrm{SFG}} \propto I_{\mathrm{vis}} I_{\mathrm{IR}} |\chi_{\mathrm{eff}}^{(2)}|^2 \tag{1}$$

$\chi_{\mathrm{eff}}^{(2)}$ is the effective second-order nonlinear susceptibility of the interface, and I_{vis} and I_{IR} are the intensities of the visible and IR incident light fields, respectively. In this case, $\chi_{\mathrm{eff}}^{(2)}$ is dominated by its resonant contribution. Therefore, $\chi_{\mathrm{eff}}^{(2)}$ can be therefore be expressed as a resonant term $\chi_{\mathrm{R}}^{(2)}$ according to

$$\chi_{\mathrm{R}}^{(2)} = N_{\mathrm{ads}} \langle \beta_{ijk,q} \rangle \tag{2}$$

In this expression, N_{ads} is the number of adsorbates at the surface or interface, and $\langle \beta_{ijk,q} \rangle$ is the ensemble orientational average of the molecular hyperpolarizability tensor. The hyperpolarizability tensor is expressed as the product of the polarizability derivative and dipole derivatives of each normal mode, q, according to

$$\beta_{ijk,q} \propto \frac{\partial \alpha_{ij}}{\partial Q_q} \frac{\partial \mu_k}{\partial Q_q} \tag{3}$$

The molecular hyperpolarizability is then rotated from molecular frame coordinates (i, j, k) to the lab frame coordinates (I, J, K) to obtain the second-order tensor $\chi_{IJK}^{(2)}$ using a $Z-Y-Z$ Euler transformation matrix according to

$$\chi_{IJK,q}^{(2)} = N \sum_{i,j,k} \langle R_{Ii} R_{Jj} R_{Kk} \rangle \beta_{ijk,q} \tag{4}$$

The molecular orientation is defined by a "tilt" angle, θ, and "twist" angle, ψ, (refer to Figure S9 in the Supporting Information), and we average the in-plane rotation, ϕ, assuming a rotationally isotropic noninteracting surface by integrating from 0 to 2π. The ssp polarization combination used in this work is defined by

$$\chi_{\mathrm{ssp}}^{(2)} = L_{yy}(\omega_{\mathrm{SFG}}) L_{yy}(\omega_{\mathrm{vis}}) L_{zz}(\omega_{\mathrm{IR}}) \sin \alpha_{\mathrm{IR}} \chi_{yyz} \tag{5}$$

The ssp polarization combination is designated s-polarized SFG, s-polarized visible, and p-polarized IR beams, where "p" designates a light field polarization that is parallel to the plane of incidence and "s" designates a light field polarization that is perpendicular to the plane of incidence.

3. METHODS

A. Functionals and Basis Sets. The computational methods used in this work have been previously described in the literature[3,4,55] and provide a starting point for our benchmarking study. The DFT calculations were preformed with the Gaussian 09, revision D.01 package.[71] For each combination of functional and basis set, geometry optimizations followed by frequency calculations were performed to obtain harmonic vibrational frequencies along with dipole derivatives and polarizability derivatives with respect to each vibrational mode, using the keywords "freq=raman iop(7/33=1)". Forthcoming work will investigate applying anharmonic approximations to vibrational frequencies and dipole and polarizability derivatives for SFG simulations. We assessed the popular DFT pure (specifically, local and gradient-corrected exchange−correlation) functionals PBE[72,73] and BP86[74,75] as well as the hybrid functionals B3LYP,[74,76,77] B97-1,[78] M06,[79] PBE0,[80] M06-2X,[79] and ωB97X-D.[81] These functionals were paired with Pople basis sets (6-31G(d), 6-31G(d,p), 6-311G(d,p), and 6-311++G(d,p))[82,83] and Dunning basis sets (cc-pVTZ[84] and augmented versions aug-cc-pVDZ[85] and aug-cc-pVTZ).[84]

The computed Raman intensity spectra given in the Supporting Information were generated using Gaussian calculations of Raman activities. The conversion of Raman activities (S_i) to relative intensities (R_i), in order to directly compare to experiment, is as follows[86−89]

DOI: 10.1021/acs.jpcb.5b09769
J. Phys. Chem. B XXXX, XXX, XXX−XXX

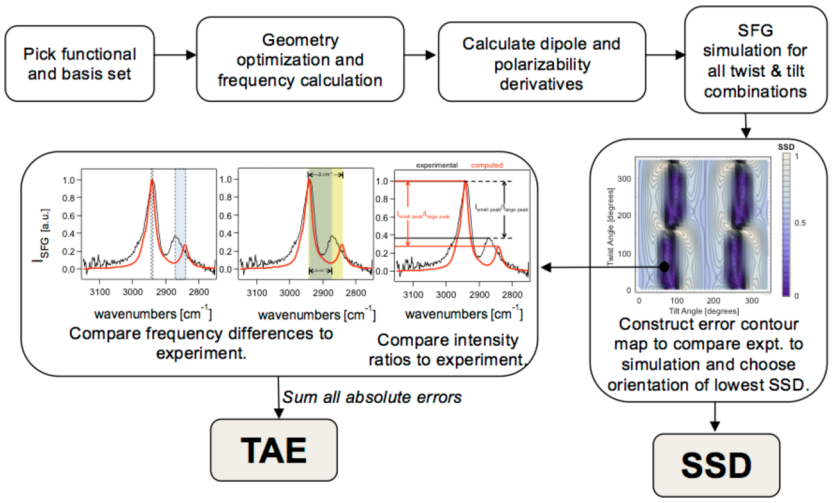

Figure 2. Schematic summary of the benchmarking analyses.

$$R_i = \frac{(2\pi)^4}{45}(\nu_0 - \nu_i)^4 \times \frac{h}{8\pi^2 c\nu_i\left(1 - \exp\left(-\frac{h\nu_i c}{kT}\right)\right)} \times S_i \tag{6}$$

where ν_i is the frequency of the ith band and ν_0 is the incident excitation wavelength, which was 532 nm, and T is the temperature of 298 K. We applied a 1 cm^{-1} Lorentzian broadening to the intensities.

B. DFT Calculations and SFG Simulations. We refer to the computational method from our recently published work[55] in order to simulate the ssp-polarized SFG spectra of *trans*-β-IEPOX and its d_2-isotopologue. The normalized computed IR spectra with no broadening are given in the Supporting Information in Figure S4, and normalized computed Raman spectra with 1 cm^{-1} Lorentzian broadening are given in Figure S5 in the Supporting Information. Briefly, we compute $\beta_{ijk,q}$ using a given functional and basis set using eq 3. This hyperpolarizability is then projected from the molecular frame to the lab frame for a given tilt and twist angle combination to obtain $(\chi^{(2)}_{ijk,q}(\varphi,\psi,\theta))$. The effective nonlinear susceptibility, χ_{eff}, is then computed, where a Lorentzian function of 12 cm^{-1} is applied to account for inhomogeneous broadening and the resolution of our spectrometer. We simulate SFG spectra for all combinations of tilt and twist angles of the C_{3v} symmetry axis of the methyl group (see the following section), ranging from 0 to 360° in 10° increments, as described in our earlier work.[55] The frequency scaling factors used in the best-matching ssp-polarized SFG simulations are displayed in Table S1. Frequency scaling factors were determined by matching the computed vibrational frequency corresponding to the computed highest signal intensity with the experimental vibrational frequency corresponding to the highest experimental signal intensity measured in the SFG and IR spectra of *trans*-β-IEPOX (see Table S1). Overall, we find that these frequency scaling factor results agree well with the work of Scott and Radom comparing scaling factors for a series of small molecules including hydrocarbons.[90] Fermi resonances were not included in this study, as explained in our previous work.[55] Overtones and combination bands were also not incorporated in the simulation because the corresponding anharmonic IR intensities were less than about 5% of the anharmonic C−H fundamental IR intensities.

C. Sum of Squared Differences (SSD) and Total Absolute Error (TAE). Figure 2 provides a summary of the procedure used for determining SSD and TAE values. For each twist and tilt angle combination, the SSD between the computed and the experimental ssp-polarized SFG spectrum is calculated. Contour error plots are then constructed from these difference values in order to visually identify the orientation of best match for further analysis (as described previously[55]). Here, we computed the SSD using the various combinations of functionals and basis sets described above. SSD values are helpful for quantifying which molecular orientations yield best matches to experiment for a particular functional and basis set combination; however, it is difficult to compare matches across different computational methods using the SSD values alone. To further identify best spectral matches while eliminating possible false-positives, we used the ratios of the SFG signal intensities and their frequencies to determine the ratio of the computed high- and low-intensity peaks, as well as the difference of the computed frequencies at which the high- and the low-intensity peaks occur for the tilt and twist angle combination that yields the lowest SSD value for a given functional/basis set combination. We then compared those values from the DFT calculations with the corresponding intensity ratio and frequency difference from experiment. We then assume that the best functional corresponds to the one that exhibits the smallest TAE between the computed and the experimental intensity and frequency ratios. More details are given in sections S7 and S8 in the Supporting Information

D. IR and Raman Spectroscopy. The IR spectrum (given in the Supporting Information Figures S1 and S4) of a thin film of *trans*-β-IEPOX was recorded at room temperature with 2 cm^{-1} resolution on a Bruker Tensor 37 FTIR spectrometer equipped with a mid-IR detector and KBr beam splitter. For this spectrum, a drop of the neat liquid compound was placed between two NaCl windows and measured in transmission mode.

The Raman spectrum of neat *trans*-β-IEPOX (given in the Supporting Information Figures S2 and S5) was measured using a HORIBA LabRAM HR Evolution Confocal Raman System Acton TriVista CRS confocal Raman system. Spectra of pure liquid samples were collected using an inverted microscope system with a 10× long-range objective lens at an excitation wavelength of 532 nm (600 gr/mm grating). Laser

DOI: 10.1021/acs.jpcb.5b09769
J. Phys. Chem. B XXXX, XXX, XXX−XXX

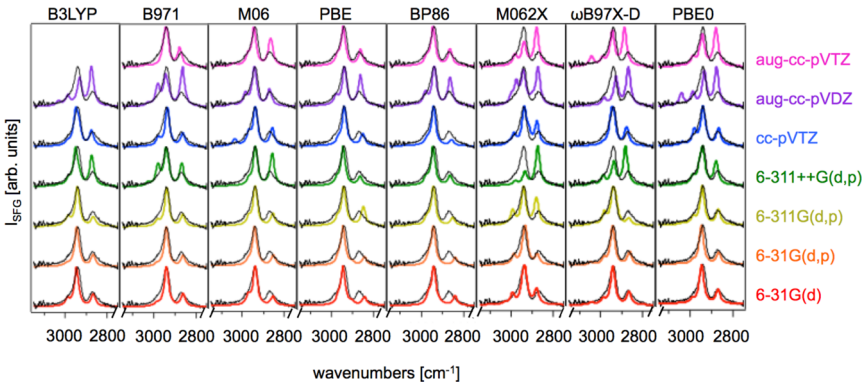

Figure 3. Best-matching simulated spectra (colored traces) for all functionals and basis sets compared to experiment (black trace).

Table 1. TAE Values for the Harmonic Vibrational Frequency SFG Simulations

basis set/functional	BP86	PBE	PBE0	B3LYP	B97-1	M06	M06-2X	ωB97x-D
6-31G(d)	46.6	64.3	11.0	15.4	15.4	24.9	35.1	11.3
6-31G(d,p)	74.4	64.3	21.6	7.60	17.9	34.7	35.7	17.3
6-311G(d,p)	47.7	42.0	7.20	6.20	15.4	26.1	24.4	7.20
6-311++G(d,p)	20.0	21.5	18.2	15.6	4.00	24.0	27.3	33.0
cc-pVTZ	25.1	35.2	7.50	14.4	15.0	21.5	24.3	18.4
aug-cc-pVDZ	8.20	14.2	31.1	36.9	18.9	5.60	12.3	38.0
aug-cc-pVTZ	21.1	21.4	23.0		18.3	16.3	25.0	36.9

power was attenuated to 25% in order to avoid burning the sample. For these measurements, CCD exposure times of 60 s were used, and spectra were averaged to improve signal-to-noise. Spectra were smoothed and baseline-corrected using the LabSpec 6 spectroscopy suite.

4. RESULTS AND DISCUSSION

A. Conformational Analysis Predicts All O-Atoms of *trans-β*-IEPOX Point to the Same Side. Although *trans-β*-IEPOX contains a rigid epoxide ring, significantly restricting the rotational degrees of freedom of the methylene groups, there are various possible conformations. We therefore tested five different structures corresponding to different conformations and simulated their SFG spectra using B3LYP/6-311G(d,p), and these results are given in section S3 in the Supporting Information. The lowest-energy conformation that also corresponded to the best-matching spectrum was chosen to perform the benchmark assessment for both *trans-β*-IEPOX and its d_2-isotopologue. As detailed in the Supporting Information, the conformation resulting in the best spectra match corresponds to a largely trans-configured system of methylene/OH groups (see Figure S3) in which all oxygen atoms point to the same side, that is, toward the fused silica surface used in the experiment. This result is consistent with the fact that *trans-β*-IEPOX contains an epoxide ring and two hydroxyl groups, which can hydrogen bond to the Si−OH groups of the silica substrate, thus steering the molecule toward a preferred angle.

B. SSD/TAE Method Identifies Which Hybrid Functionals and Basis Sets Yield the Best Spectral Matches with Computed Frequencies for the SFG Spectra of *trans-β*-IEPOX. Having identified a seemingly preferred conformation for *trans-β*-IEPOX for one functional/basis set combination, we proceeded to compute, for a series of functional/basis set combinations, the SFG spectra for all tilt and twist angle combinations in 10° increments. Contour plots of the SSD were then used to visually identify the range in tilt and twist angles resulting in the best spectral match for each functional/basis set combination. Figure 3 shows the experimental spectrum along with the best-matching spectra obtained from the calculations, with the quantitative comparison given in Tables S2−S5.

We find that a majority of the largest mismatches arising in the calculations are associated with the PBE and BP86 pure functionals with the Pople basis sets evaluated. This result is not surprising in that pure functionals poorly predict some properties such as polarizabilities through the lack of any Hartree−Fock exact exchange component.[42,43,91] Hybrid functionals also tend to perform better in predicting IR intensities.[92] In fact, PBE has been recently shown by Rowley and coworkers[43] to systematically overestimate polarizabilities in their benchmarking study, which may result in large differences in SFG intensities. However, we do observe improvements in the spectral matches when pairing the pure functionals with the Dunning basis sets, as seen in Table 1. When combined with a large basis set, however, the local functionals are a good option for molecules where hybrid functionals would be too expensive.

To quantify these observations, we calculated the SSD values for each simulated spectrum in Figure 2 (tabulated in Table S2) and plotted them against the TAE values, obtained as described in section 3C. According to this analysis, we expect that the best-performing functional/basis set combination would result in small SSD and TAE values. The results are shown in Figure 4A. We find dramatic improvements in TAE values with the hybrid PBE0 functional compared to those with the pure PBE counterpart, showcasing the potential importance of incorporating partial Hartree−Fock exchange treatment. In fact, we find that the use of the hybrid functionals B97-1, B3LYP, PBE0, and ωB97X-D lead to the smallest TAE values, particularly with the Pople basis sets. Both B3LYP and BP97-1 were also found to perform well in predicting frequencies harmonically in a previous study.[93] We note that by including diffuse functions to the basis set (6-311++G(d,p)), the four hybrid functionals

DOI: 10.1021/acs.jpcb.5b09769
J. Phys. Chem. B XXXX, XXX, XXX−XXX

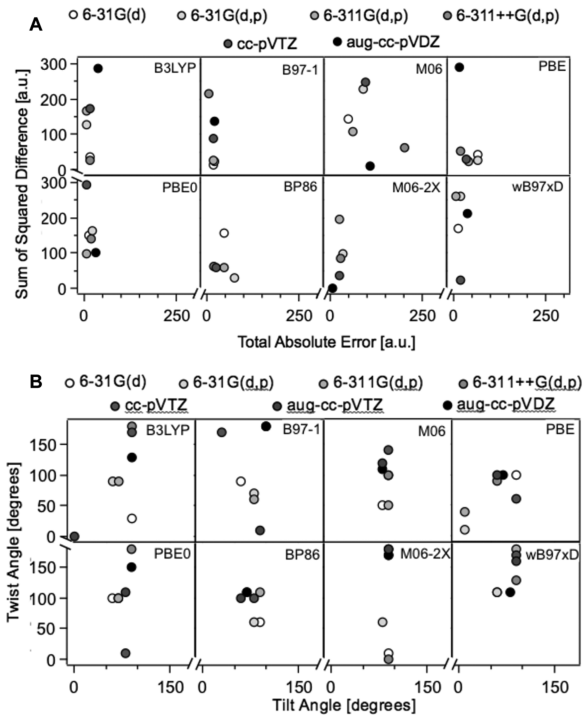

Figure 4. TAE versus SSD plots as a function of basis set for each functional (A) and orientations corresponding to spectra that match best with experiment for all functionals and basis sets (B).

studied yield drastic differences in the SFG spectra, specifically in terms of SFG intensities, which do not match well with experiment. Similarly, we obtain poor matches when pairing the hybrid functionals with the Dunning basis sets.

We find that with a small basis set, hybrid functionals outperform the pure functionals, whereas with a large basis set, the pure functionals outperform the hybrid functionals. This result indicates that the pure functionals improve in their description of spectral quantities systematically with basis set, whereas the hybrid functionals, which include semiemprical parameters, do not. There may also be a significant amount of fortuitous cancellation of errors. Specifically, the error in the frequencies from the pure functionals predicting geometries incorrectly may be canceled out by the error in the harmonic approximation.[52,94]

We observe roughly similar TAE values ranging in between those obtained for the pure and the hybrid functionals for the M06 and M06-2X functionals for all basis sets surveyed. M06-2X includes two times the Hartree−Fock exchange component compared to M06. These results indicate that an increase in exchange may not necessarily lead to drastic improvements in the quality of the spectral match. This parameter as well as others should be taken into account when parametrizing new functionals, as found recently for IR spectra.[93,95] Moreover, we conclude that there is no overall distinct correlation between the basis set size and the quality of the spectral match when it comes to predicting the SFG response for *trans*-β-IEPOX.

C. Calculated Tilt Angle of *trans*-β-IEPOX is Largely Independent of the Functional and Basis Set, Whereas the Twist Angle Is Not. Following the identification of functionals and basis sets that produce good spectral matches between the simulations and the experiment, we determined the molecular tilt and twist angles corresponding to the best-matching spectrum for each functional/basis set combination. The results are shown in Figure 4B. We find that a majority of the functional/basis set combinations predicts orientations of about 60−90° for the CH_3 tilt angle and a range of 50−130° for the CH_3 twist angle. A few combinations compute best-fitting spectra outside of this range of orientations. We conclude that the orientation analysis alone does not provide a venue for identifying the best functional for simulating the SFG responses of *trans*-β-IEPOX, at least for the twist angles.

D. SFG Spectrum of d_2-*trans*-β-IEPOX is Properly Simulated with the Same Method. Our previously published work shows that the computational approach that we employ produces reasonably well-matching SFG spectra from computation and experiment for not only *trans*-β-IEPOX (Figure 1A) alone but also for d_2-*trans*-β-IEPOX (Figure 1B). We interpreted this result to point toward a high level of reliability of our computed spectra. Thus, we expect here that similar limitations for model chemistries and basis sets that apply for the unlabeled compound should also apply to the d_2-isotopologue. Testing this hypothesis is important, given the coherent nature of SFG.

We test the functional basis set combination that gives the best and worst matches to experiment against the ssp-polarized SFG spectrum of d_2-*trans*-β-IEPOX (Figure 1B) at the vapor/silica interface. This compound is predicted to exhibit a similar orientation to its hydrogenated analogue;[55] therefore, it serves as a basis for comparison. SFG spectra from B3LYP/6-311G(d,p), as well as ωB97X-D with 6-31G(d) and 6-31G(d,p), all show agreement for the unlabeled *trans*-β-IEPOX, as shown by small TAE values in Table 1. The same results are obtained for the deuterated isotopologue, as shown in Figure 5. We also computed SFG spectra for the BP86/6-31G(d) and 6-31G(d,p) combination, which resulted in some of the largest TAE values for hydrogenated IEPOX. Our computed spectra with d_2-IEPOX showed similar poor fits to experiment, as shown in Figure 5A and B. We predict that the hybrid functionals and Pople basis sets identified here for the unlabeled and the labeled epoxide studied may be the best-

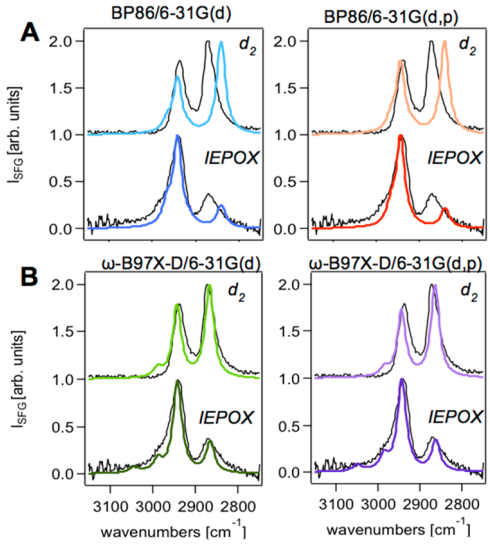

Figure 5. Simulated spectra using BP86/6-31G(d) and 6-31G(d,p) (A) and simulated spectra using ω-B97X-D/6-31G(d) and 6-31G(d,p) (B). The experimental spectrum is the black trace, and the simulated spectra are given by the colored traces. Offset for clarity are the d_2-IEPOX spectra.

DOI: 10.1021/acs.jpcb.5b09769
J. Phys. Chem. B XXXX, XXX, XXX−XXX

performing functional and basis sets for similarly strained, small gas-phase oxygenated hydrocarbons and their isotopologues , with B3LYP/6-311G(d,p) being the best starting point with a balance of speed and accuracy. It is unclear whether these results may be applicable to condensed-phase studies.

Our results are consistent with those from Guthmuller and co-workers, although they did not explore different basis sets.[50,51] They carried out a study comparing the orientations that yielded optimal matches to a SFG spectrum of a dodecanethiol as a function of DFT functional and found that varying the functional resulted in slight changes in the molecular tilt angle.[50] Similarly, in a different study, they carried out a similar assessment of DFT functionals for computing the SFG spectrum of *p*-nitrothiophenol and 2,4-dinitroanaline,[51] finding that B3LYP/6-311++G(d,p) yielded better matches to experiment than BP86 and PBE0 and a few other functionals that were not tested in this study.

5. CONCLUSIONS

The C−H stretching region is spectroscopically important because it offers extremely strong SFG intensities, compared to other frequency regions, and can be used to probe interfacial dynamics of a large class of systems. However, SFG spectra are difficult to simulate in the C−H stretching region because it is very congested with many vibrational modes, anharmonicities, overtones, combination bands, and/or Fermi resonances that are difficult to resolve. Yet, SFG simulations are essential to assign experimental results for interfaces that produce spectra that are highly congested. By benchmarking popular DFT functionals and basis sets in computing harmonic vibrational SFG spectra of environmentally relevant epoxides at the vapor/silica interface, we rigorously investigated which combination of functional and basis set performs better. Our work shows that increasing the basis set generally improves the agreement between experiments and calculations, based on pure functionals such as PBE and BP86. However, we do not observe systematic improvement by increasing the size of the basis set for calculations based on hybrid functionals such as B3LYP, ωB97X-D, PBE0, B97-1, M06, and M06-2X.

■ ASSOCIATED CONTENT

Supporting Information

The Supporting Information is available free of charge on the ACS Publications website at DOI: 10.1021/acs.jpcb.5b09769.

Experimental and computed IR spectra, conformation structure assessment, frequency scaling factors, summary of our frequency and SFG intensity assessments, and graphical depiction of the molecular orientation (PDF)

■ AUTHOR INFORMATION

Corresponding Authors

*E-mail: geigerf@chem.northwestern.edu. Phone: (847) 467-6553. Fax: (847) 491-7713 (F.M.G.).

*E-mail: victor.batista@yale.edu. Phone: (203) 432-6672. Fax: (203) 432-6144 (V.S.B.).

Notes

The authors declare no competing financial interest.

■ ACKNOWLEDGMENTS

H.M.C. acknowledges support from a National Science Foundation (NSF) graduate research fellowship and the Institute for Sustainability and Energy at Northwestern (ISEN). B.R. acknowledges support from the National Science Foundation Graduate Research Fellowship under Grant No. DGE-1122492. M.A.U. gratefully acknowledges support from a National Aeronautics and Space Administration Earth and Space (NASA ESS) Fellowship. F.M.G. and R.J.T. acknowledge support from the National Science Foundation (NSF CHE1212692 and SP0017343). V.S.B. acknowledges supercomputer time from NERSC and the Yale High Performance Computing Center, and support from NSF Grant CHE-1465108. This work made use of the confocal Raman system in the Keck-II facility (NUANCE Center, Northwestern University) and the FTIR spectrometer in the Integrated Molecular Structure Education and Research Center (IMSERC, Northwestern University).

■ REFERENCES

(1) Fu, L.; Liu, J.; Yan, E. C. Y. Chiral Sum Frequency Generation Spectroscopy for Characterizing Protein Secondary Structures at Interfaces. *J. Am. Chem. Soc.* **2011**, *133*, 8094−8097.

(2) Fu, L.; Wang, Z.; Yan, E. C. Y. Chiral Vibrational Structures of Proteins at Interfaces Probed by Sum Frequency Generation Spectroscopy. *Int. J. Mol. Sci.* **2011**, *12*, 9404−9425.

(3) Fu, L.; Xiao, D.; Wang, Z.; Batista, V. S.; Yan, E. C. Y. Chiral Sum Frequency Generation for in Situ Probing Proton Antiparallel Beta-Sheets at Interfaces. *J. Am. Chem. Soc.* **2013**, *135*, 3592−3598.

(4) Xiao, D.; Fu, L.; Liu, J.; Batista, V. S.; Yan, E. C. Y. Amphiphilic Adsorption of Human Islet Amyloid Polypeptide Aggregrates to Lipid/Aqueous Interfaces. *J. Mol. Biol.* **2012**, *421*, 537−547.

(5) Yan, E. C. Y.; Fu, L.; Wang, Z.; Liu, W. Biological Macromolecules at Interfaces Probed by Chiral Vibrational Sum Frequency Generation Spectroscopy. *Chem. Rev.* **2014**, *114*, 8471−8498.

(6) Cremer, P. S.; Su, X.; Shen, Y. R.; Somorjai, G. A. Ethylene Hydrogenation on Pt(111) Monitored in Situ at High Pressures Using Sum Frequency Generation. *J. Am. Chem. Soc.* **1996**, *118*, 2942−2949.

(7) Achtyl, J. L.; Buchbinder, A. M.; Geiger, F. M. Hydrocarbon on Carbon: Coherent Vibrational Spectroscopy of Toluene on Graphite. *J. Phys. Chem. Lett.* **2012**, *3*, 280−282.

(8) Ebben, C. J.; Strick, B. F.; Upshur, M. A.; Chase, H. M.; Achtyl, J. L.; Thomson, R. J.; Geiger, F. M. Towards the Identification of Molecular Constituents Associated with the Surfaces of Isoprene-Derived Secondary Organic Aerosol (Soa) Particles. *Atmos. Chem. Phys.* **2014**, *14*, 2303−2314.

(9) Stokes, G. Y.; Buchbinder, A. M.; Gibbs-Davis, J. M.; Scheidt, K. A.; Geiger, F. M. Heterogenous Ozone Oxidation Reactions of 1-Pentene, Cyclopentene, Cyclohexene, and Menthenol Derivative Studied by Sum Frequency Generation. *J. Phys. Chem. A* **2008**, *112*, 11688−11698.

(10) Stokes, G. Y.; Buchbinder, A. M.; Gibbs-Davis, J. M.; Scheidt, K. A.; Geiger, F. M. Chemically Diverse Environmental Interfaces and Their Reactions with Ozone Studied by Sum Frequency Generation. *Vib. Spectrosc.* **2009**, *50*, 86−98.

(11) Stokes, G. Y.; Chen, E. H.; Buchbinder, A. M.; Paxton, W. F.; Keeley, A.; Geiger, F. M. Atmospheric Heterogeneous Stereochemistry. *J. Am. Chem. Soc.* **2009**, *131*, 13733−13737.

(12) Stokes, G. Y.; Gibbs-Davis, J. M.; Boman, F. C.; Stepp, B. R.; Condie, A. G.; Nguyen, S. T.; Geiger, F. M. Making "Sense" of DNA. *J. Am. Chem. Soc.* **2007**, *129*, 7492−7493.

(13) Upshur, M. A.; Strick, B. F.; McNeill, V. F.; Thomson, R. J.; Geiger, F. M. Climate-Relevant Physical Properties of Molecular Constituents for Isoprene-Derived Secondary Organic Aerosol Material. *Atmos. Chem. Phys.* **2014**, *14*, 10731−10740.

(14) Walter, S. R.; Geiger, F. M. DNA on Stage: Showcasing Oligonucleotides at Surfaces and Interfaces with Second Harmonic and Vibrational Sum Frequency Generation. *J. Phys. Chem. Lett.* **2010**, *1*, 9−15.

(15) Hall, S. A.; Jena, K. C.; Covert, P. A.; Roy, S.; Trudeau, T. G.; Hore, D. K. Molecular Level Surface Structure from Nonlinear Vibrational Spectroscopy Combined with Simulations. *J. Phys. Chem. B* **2014**, *118*, 5617.
(16) Yang, M.; Somorjai, G. A. Adsorption and Reactions of C6 Hydrocarbons at High Pressures on Pt(111) Single-Crystal Surfaces Studied by Sum Frequency Generation Vibrational Spectroscopy: Mechanisms of Isomerization and Dehydrocyclization of N-Hexane. *J. Am. Chem. Soc.* **2004**, *126*, 7698−7708.
(17) Su, X.; Cremer, P. S.; Shen, Y. R.; Somorjai, G. A. High-Pressure Co Oxidation on Pt(111) Monitored with Infrared-Visible Sum Frequency Generation (Sfg). *J. Am. Chem. Soc.* **1997**, *119*, 3994−4000.
(18) Somorjai, G. A.; McCrea, K. R. Sum Frequency Generation: Surface Vibrational Spectroscopy Studies of Catalytic Reactions on Metal Single-Crystal Surfaces. *Adv. Catal.* **2000**, *45*, 385−438.
(19) Brown, M. G.; Walker, R. A.; Raymond, E. A.; Richmond, G. L. Vibration Sum-Frequency Spectroscopy of Alkane/Water Interfaces: Experiment and Theoretical Simulation. *J. Phys. Chem. B* **2003**, *107*, 237−244.
(20) Sierra-Hernandez, M. R.; Allen, H. C. Incorportation and Exclusion of Long Chain Alkyl Halides in Fatty Acid Monolayers at the Air-Water Interface. *Langmuir* **2010**, *26*, 18806−18816.
(21) Fu, L.; Zhang, H.; Wei, Z.-H.; Wang, H.-F. Intrinsic Chirality and Prochirality at Air/R-(+)- and S-(−)-Limonene Interfaces: Spectral Signatures with Interference Chiral Sum-Frequency Generation Vibrational Spectroscopy. *Chirality* **2014**, *26*, 509−520.
(22) Sekino, H.; Maeda, Y.; Kamiya, M.; Hirao, K. Polarizability and Second Hyperpolarizability Evaluation of Long Molecules by the Density Functional Theory with Long-Range Correction. *J. Chem. Phys.* **2007**, *126*, 014107.
(23) Schleeger, M.; Nagata, Y.; Bonn, M. Quantifying Surfactant Alkyl Chain Orientation and Conformational Order from Sum Frequency Generation Spectra of Ch Modes at the Surfactant-Water Interface. *J. Phys. Chem. Lett.* **2014**, *5*, 3737−3741.
(24) Conboy, J. C.; Messmer, M. C.; Richmond, G. L. Dependence of Alkyl Chain Conformation of Simple Ionic Surfactants on Head Group Functionality as Studied by Vibrational Sum-Frequency Spectroscopy. *J. Phys. Chem. B* **1997**, *101*, 6724−6733.
(25) Smiley, B. L.; Richmond, G. L. Alkyl Chain Ordering of Asymmetric Phosphatidylcholines Adsorbed at a Liquid-Liquid Interface. *J. Phys. Chem. B* **1999**, *103*, 653−659.
(26) Conboy, J. C.; Messmer, M. C.; Richmond, G. L. Effect of Alkyl Chain Length on the Conformation and Order of Simple Ionic Surfactants Adsorbed at the D2o/Ccl4 Interface as Studied by Sum-Frequency Vibrational Spectroscopy. *Langmuir* **1998**, *14*, 6722−6727.
(27) Geiger, F. M. Second Harmonic Generation, Sum Frequency Generation, and X(3): Dissecting Environmental Interfaces with a Nonlinear Optical Swiss Army Knife. *Annu. Rev. Phys. Chem.* **2009**, *60*, 61−83.
(28) Capouet, M.; Peeters, J.; Noziere, B.; Muller, J.-F. Alpha-Pinene Oxidation by OH: Simulations of Laboratory Experiments. *Atmos. Chem. Phys.* **2004**, *4*, 2285−2311.
(29) Jimenez, J. L.; Canagaratna, M. R.; Donahue, N. M.; Prevot, A. S. H.; Zhang, Q.; Kroll, J. H.; DeCarlo, P. F.; Allan, J. D.; Coe, H.; Ng, N. L.; et al. Evolution of Organic Aerosols in the Atmosphere. *Science* **2009**, *326*, 1525−1529.
(30) Kroll, J. H.; Seinfeld, J. H. Chemistry of Secondary Organic Aerosol: Formation and Evolution of Low-Volatility Organics in the Atmosphere. *Atmos. Environ.* **2008**, *42*, 3593−2624.
(31) Ebben, C. J.; Shrestha, M.; Martinez, I. S.; Corrigan, A. L.; Frossard, A. A.; Song, W. W.; Worton, D. R.; Petäjä, T.; Williams, J.; Russell, L. M.; et al. Organic Constituents on the Surfaces of Aerosol Particles from Southern Finland, Amazonia, and California Studied by Vibrational Sum Frequency Generation. *J. Phys. Chem. A* **2012**, *116*, 8271−8290.
(32) Mahapatra, M.; Tysoe, W. T. Chemisorptive Enantioselectivity of Chiral Epoxides on Tartaric-Acid Modified Pd(111): Three-Point Bonding. *Phys. Chem. Chem. Phys.* **2015**, *17*, 5450−5458.
(33) Gao, F.; Wang, Y.; Li, Z.; Furlong, O.; Tysoe, W. T. Enantioselective Reactions on a Au/Pd(111) Surface Alloy with Coadsorbed Chiral 2-Butanol and Propylene Oxide. *J. Phys. Chem. C* **2008**, *112*, 3362−3372.
(34) Stacchiola, D.; Burkholder, L.; Tysoe, W. T. Enantioselective Chemisorption on a Chirally Modified Surface in Ultrahigh Vacuum: Adsorption of Propylene Oxide on 2-Butoxide-Covered Palladium(111). *J. Am. Chem. Soc.* **2002**, *124*, 8984−8989.
(35) Guthmuller, J. Assessment of Td-Dft and Cc2Methods for the Calculation of Resonance Raman Intensities: Application to O-Nitrophenol. *J. Chem. Theory Comput.* **2011**, *7*, 1082−1089.
(36) Lee, C. M.; Mohamed, N. M. A.; Watts, H. D.; Kubicki, J. D.; Kim, S. H. Sum-Frequency-Generation Vibration Spectroscopy and Density Functional Theory Calculations with Dispersion Corrections (Dft-D2) for Cellulose 1a and 1b. *J. Phys. Chem. B* **2013**, *117*, 6681−6692.
(37) Zheng, R.-h.; Wei, W.-m.; Jing, Y.-y.; Liu, H.; Shi, Q. Theoretical Study of Doubly Resonant Sum-Frequency Vibrational Spectroscopy for 1,1′-Bi-2-Naphthol Molecules on Water Surface. *J. Phys. Chem. C* **2013**, *117*, 11117−11123.
(38) Ishiyama, T.; Imamura, T.; Morita, A. Theoretical Studies of Structures and Vibrational Sum Frequency Generation Spectra at Aqueous Interfaces. *Chem. Rev.* **2014**, *114*, 8447−8470.
(39) Sulpizi, M.; Salanne, M.; Sprik, M.; Gaigeot, M.-P. Vibrational Sum Frequency Generation Spectroscopy of the Water Liquid−Vapor Interface from Density Functional Theory-Based Molecular Dynamics Simulations. *J. Phys. Chem. Lett.* **2013**, *4*, 83−87.
(40) Lee, C. M.; Mohamed, N. M. A.; Watts, H. D.; Kubicki, J. D.; Kim, S. H. Sum-Frequency-Generation Vibration Spectroscopy and Density Functional Theory Calculations with Dispersion Corrections (Dft-D2) for Cellulose Iα and Iβ. *J. Phys. Chem. B* **2013**, *117*, 6681−6692.
(41) Cecchet, F.; Lis, D.; Guthmuller, J.; Champagne, B.; Fonder, G.; Mekhalif, Z.; Caudano, Y.; Mani, A. A.; Thiry, P. A.; Peremans, A. Theoretical Calculations and Experimental Measurements of the Vibrational Response of P-Ntp Sams: An Orientational Analysis. *J. Phys. Chem. C* **2010**, *114*, 4106−4113.
(42) Hammond, J. R.; Govind, N.; Kowalski, K.; Autschbach, J.; Xantheas, S. S. Accurate Dipole Polarizabilities for Water Clusters N = 2−12 at the Coupled-Cluster Level of Theory and Benchmarking of Various Density Functionals. *J. Chem. Phys.* **2009**, *131*, 214103.
(43) Hickey, A. L.; Rowley, C. N. Benchmarking Quantum Chemical Methods for the Calculation of Molecular Dipole Moments and Polarizabilities. *J. Phys. Chem. A* **2014**, *118*, 3678−3687.
(44) Patton, D. C.; Porezag, D.; Pederson, M. R. Simplified Generalized-Gradient Approximation and Anharmonicity: Benchmark Calculations on Molecules. *Phys. Rev. B: Condens. Matter Mater. Phys.* **1997**, *55*, 7454−7459.
(45) Valdes, H.; Pluhackova, K.; Pitonak, M.; Rezac, J.; Hobza, P. Benchmark Database on Isolated Small Peptides Containing an Aromatic Side Chain: Comparison between Wave Function and Density Functional Theory Methods and Empiracle Force Field. *Phys. Chem. Chem. Phys.* **2008**, *10*, 2747−2757.
(46) Barone, V.; Biczysko, M.; Bloino, J. Fully Anharmonic Ir and Raman Spectra of Medium-Size Molecular Systems: Accuracy and Interpretation. *Phys. Chem. Chem. Phys.* **2014**, *16*, 1759−1787.
(47) Carnimeo, I.; Puzzarini, C.; Tasinato, N.; Stoppa, P.; Charmet, A. P.; Biczysko, M.; Cappelli, C.; Barone, V. Anharmonic Theoretical Simulations of Infrared Spectra of Halogenated Organic Compounds. *J. Chem. Phys.* **2013**, *139*, 074310.
(48) Puzzarini, C.; Biczysko, M.; Bloino, J.; Barone, V. Accurate Spectroscopic Characterization of Oxirane: A Valuable Route to Its Identification in Titan's Atmosphere and the Assignment of Unidentified Infrared Bands. *Astrophys. J.* **2014**, *785*, 107.
(49) Cheeseman, J. R.; Frisch, M. J. Basis Set Dependence of Vibrational Raman and Raman Optical Activity Intensities. *J. Chem. Theory Comput.* **2011**, *7*, 3323−3334.
(50) Cecchet, F.; Lis, D.; Caudano, Y.; Mani, A. A.; Peremans, A.; Champagne, B.; Guthmuller, J. Density Functional Theory-Based

DOI: 10.1021/acs.jpcb.5b09769
J. Phys. Chem. B XXXX, XXX, XXX−XXX

Simulations of Sum Frequency Generation Spectra Involving Methyl Stretching Vibrations: Effect of the Molecular Model on the Deduced Molecular Orientation and Comparison with an Analytical Approach. *J. Phys.: Condens. Matter* **2012**, *24*, 124110−124119.

(51) Guthmuller, J.; Cecchet, F.; Lis, D.; Caudano, Y.; Mani, A. A.; Thiry, P. A.; Peremans, A.; Champagne, B. Theoretical Simulation of Vibrational Sum-Frequency Generation Spectra from Density Functional Theory: Application of p-Nitrothiophenol and 2,4-Dinitroanaline. *ChemPhysChem* **2009**, *10*, 2132−2142.

(52) Sebek, J.; Knaanie, R.; Albee, B.; Potma, E. O.; Gerber, R. B. Spectroscopy of the C−H Stretching Vibrational Band in Selected Organic Molecules. *J. Phys. Chem. A* **2013**, *117*, 7442−7452.

(53) Sebek, J.; Pele, L.; Potma, E. O.; Gerber, R. B. Raman Spectra of Long Chain Hydrocarbons: Anharmonic Calculations, Experiment and Implications for Imaging of Biomembranes. *Phys. Chem. Chem. Phys.* **2011**, *13*, 12724−12733.

(54) Chen, Y.; Morisawa, Y.; Futami, Y.; Czarnecki, M. A.; Wang, H.-S.; Ozaki, Y. Combined Nir/Ir and Density Functional Theory Calculations Analysis of the Solvent Effects on Frequencies and Intensities of the Fundamental and Overtones of the C═O Stretching Vibrations of Acetone and 2-Hexanone. *J. Phys. Chem. A* **2014**, *118*, 2576−2583.

(55) Chase, H. M.; Psciuk, B. T.; Strick, B. F.; Thomson, R. J.; Batista, V. S.; Geiger, F. M. Beyond Local Group Modes in Sum Frequency Generation Spectroscopy. *J. Phys. Chem. A* **2015**, *119*, 3407−3414.

(56) Choi, C. H.; Kertesz, M. Density Functional Studies of Vibrational Properties of HCN, H_2O, CH_2O, CH_4 and C_2H_4. *J. Phys. Chem.* **1996**, *100*, 16530−16537.

(57) Pecul, M.; Pawłowski, F.; Jørgensen, P.; Köhn, A.; Hättig, C. High-Order Correlation Effects on Dynamic Hyperpolarizabilities and Their Geometric Derivatives: A Comparison with Density Functional Results. *J. Chem. Phys.* **2006**, *124*, 114101.

(58) Zawada, A.; Kaczmarek-Kędziera, A.; Bartkowiak, W. On the Potential Application of Dft Methods in Predicting the Interaction-Induced Electric Properties of Molecular Complexes. Molecular H-Bonded Chains as a Case of Study. *J. Mol. Model.* **2012**, *18*, 3073−3086.

(59) Bates, K. H.; Crounse, J. D.; St. Clair, J. M.; Bennett, N. B.; Nguyen, T. B.; Seinfeld, J. H.; Stoltz, B. M.; Wennberg, P. O. Gas Phase Production and Loss of Isoprene Epoxydiols. *J. Phys. Chem. A* **2014**, *118*, 1237−46.

(60) Chan, M. N.; Surratt, J. D.; Claeys, M.; Edgerton, E. S.; Tanner, R. L.; Shaw, S. L.; Zheng, M.; Knipping, E. M.; Eddingsaas, N. C.; Wennberg, P. O.; et al. Characterization and Quantification of Isoprene-Derived Epoxydiols in Ambient Aerosol in the Southeastern United States. *Environ. Sci. Technol.* **2010**, *44*, 4590−4596.

(61) Lin, Y.-H.; Zhang, Z.; Docherty, K. S.; Zhang, H.; Budisulistiorini, S. H.; Rubitschun, C. L.; Shaw, S. L.; Knipping, E. M.; Edgerton, E. S.; Kleindienst, T. E.; et al. Isoprene Epoxydiols as Precursors to Secondary Organic Aerosol Formation: Acid-Catalyzed Reactive Uptake Studies with Authentic Compounds. *Environ. Sci. Technol.* **2012**, *46*, 250−258.

(62) Liu, Y.; Kuwata, M.; Strick, B. F.; Thomson, R. J.; Geiger, F. M.; McKinney, K. A.; Martin, S. T. Epoxydiol Isomers Account for Half of the Particle-Phase Material Produced from Isoprene Photooxidation. *Environ. Sci. Technol.* **2015**, *49*, 250−258.

(63) Surratt, J. D.; Chan, A. W. H.; Eddingsaas, N. C.; Chan, M.; Loza, C. L.; Kwan, A. J.; Hersey, S. P.; Flagan, R. C.; Wennberg, P. O.; Seinfeld, J. H. Reactive Intermediates Revealed in Secondary Organic Aerosol Formation from Isoprene. *Proc. Natl. Acad. Sci. U. S. A.* **2010**, *107*, 6640−6645.

(64) Turner, D. P.; Baglio, J. V.; Wones, A. G.; Pross, D.; Vong, R.; McVeety, B. D.; Phillips, D. L. Climate Change and Isoprene Emissions from Vegetation. *Chemosphere* **1991**, *23*, 37−56.

(65) Moad, A. J.; Simpson, G. J. A Unified Treatment of Selection Rules and Symmetry Relations for Sum-Frequency and Second Harmonic Spectroscopies. *J. Phys. Chem. B* **2004**, *108*, 3548−3562.

(66) Shen, Y. R. *The Principles of Nonlinear Optics*; Wiley-Interscience: New York, 1984; p 575.

(67) Wang, H.-F.; Gan, W.; Lu, R.; Rao, Y.; Wu, B.-H. Quantitative Spectral and Orientational Analysis in Surface Sum Frequency Generation Vibrational Spectroscopy (Sfg-Vs). *Int. Rev. Phys. Chem.* **2005**, *24*, 191−256.

(68) Boyd, R. W. *Nonlinear Optics*; Academic Press: New York, 2003.

(69) Shen, Y. R. Surfaces Probed by Nonlinear Optics. *Surf. Sci.* **1994**, *299−300*, 551.

(70) Richmond, G. L. Molecular Bonding and Interactions at Aqueous Surfaces as Probed by Vibrational Sum Frequency Spectroscopy. *Chem. Rev.* **2002**, *102*, 2693−2724.

(71) Frisch, M. J.; Trucks, G. W.; Schlegel, H. B.; Scuseria, G. E.; Robb, M. A.; Cheeseman, J. R.; Montgomery, J. J. A.; Vreven, T.; Kudin, K. N.; Burant, J. C.; et al. *Gaussian 09*, revision D.02; Gaussian, Inc.: Wallingford, CT, 2009.

(72) Perdew, J. P.; Burke, K.; Ernzerhof, M. Generalized Gradient Approximation Made Simple. *Phys. Rev. Lett.* **1996**, *77*, 3865−3868.

(73) Perdew, J. P.; Burke, K.; Ernzerhof, M. Errata: Generalized Gradient Approximation Made Simple. *Phys. Rev. Lett.* **1997**, *78*, 1396.

(74) Becke, A. D. Density-Function Thermochemistry. Iii. The Role of Exact Exchange. *J. Chem. Phys.* **1993**, *98*, 5648−5652.

(75) Perdew, J. P. Density-Functional Approximation for the Correlation Energy of the Inhomogeneous Electron Gas. *Phys. Rev. B: Condens. Matter Mater. Phys.* **1986**, *33*, 8822−8824.

(76) Lee, C.; Yang, W. S.; Parr, R. G. Development of the Colle-Salvetti Correlation-Energy Formula into a Functional of the Electron Density. *Phys. Rev. B: Condens. Matter Mater. Phys.* **1988**, *37*, 785−789.

(77) Stephens, P. J.; Devlin, F. J.; Chabalowski, C. F.; Frisch, M. J. Ab Initio Calculation of Vibrational Absorption and Circular Dichroism Spectra Using Density Functional Force Fields. *J. Phys. Chem.* **1994**, *98*, 11623−11627.

(78) Hamprecht, F. A.; Cohen, A.; Tozer, D. J.; Handy, N. C. Development and Assessment of New Exchange-Correlation Functionals. *J. Chem. Phys.* **1998**, *109*, 6264−6271.

(79) Zhao, Y.; Truhlar, D. G. The M06 Suite of Density Functionals for Main Group Thermochemistry, Thermochemical Kinetics, Noncovalent Interactions, Excited States, and Transition Elements: Two New Functionals and Systematic Testing of Four M06-Class Functionals and 12 Other Functionals. *Theor. Chem. Acc.* **2008**, *120*, 215−241.

(80) Adamo, C.; Barone, V. Toward Reliable Density Functional Methods without Adjustable Parameters: The Pbe0Model. *J. Chem. Phys.* **1999**, *110*, 6158−6169.

(81) Chai, J.-D.; Head-Gordon, M. Long-Range Corrected Hybrid Density Functionals with Damped Atom-Atom Dispersion Corrections. *Phys. Chem. Chem. Phys.* **2008**, *10*, 6615−6620.

(82) Krishnan, R.; Binkley, J. S.; Seeger, R.; Pople, J. A. Selfconsistent Molecular Orbital Methods. Xx. A Basis Set for Correlated Wave Functions. *J. Chem. Phys.* **1980**, *72*, 650−654.

(83) Francl, M. M.; Pietro, W. J.; Hehre, W. J.; Binkley, J. S.; Gordon, M. S.; DeFrees, D. J.; Pople, J. A. Self-Consistent Molecular Orbital Methods. XXIII. A Polarization-Type Basis Set for Second-Row Elements. *J. Chem. Phys.* **1982**, *77*, 3654.

(84) Kendall, R. A.; Dunning, T. H., Jr.; Harrison, R. J. Electron Affinities of the First-Row Atoms Revisited. Systematic Basis Sets and Wave Functions. *J. Chem. Phys.* **1992**, *96*, 6796−6806.

(85) Dunning, T. H., Jr. Gaussian Basis Sets for Use in Correlated Molecular Calculations. I. The Atoms Boron through Neon and Hydrogen. *J. Chem. Phys.* **1989**, *90*, 1007−1023.

(86) Polavarapu, P. L. Ab Initio Vibrational Raman and Raman Optical Activity Spectra. *J. Phys. Chem.* **1990**, *94*, 8106−8112.

(87) Krishnakumar, V.; Keresztury, G.; Sundius, T.; Ramasamy, R. Simulation of Ir and Raman Spectra Based on Scaled Dft Force Fields: A Case Study of 2-(Methylthio)Benzonitrile, with Emphasis on Band Assignment. *J. Mol. Struct.* **2004**, *702*, 9−21.

(88) Michalska, D.; Wysokinski, R. The Prediction of Raman Spectra of Platinum (Ii) Anticancer Drugs by Density Functional Theory. *Chem. Phys. Lett.* **2005**, *403*, 211−217.

DOI: 10.1021/acs.jpcb.5b09769
J. Phys. Chem. B XXXX, XXX, XXX−XXX

(89) Keresztury, G.; Holly, S.; Besenyei, G.; Varga, J.; et al. Vibrational Spectra of Monothiocarbamates-II. IR and Raman Spectra, Vibrational Assignment, Conformational Analysis and Ab Initio Calculations of S-Methyl-N,N-Dimethylthiocarbamate. *Spectrochim. Acta* **1993**, *49A*, 2007−2026.

(90) Scott, A. P.; Radom, L. Harmonic Vibrational Frequencies: An Evalutation of Hartree−Fock, Møller-Plesset, Quadratic Configuration Interaction, Density Functional Theory, and Semiempirical Scale Factors. *J. Phys. Chem.* **1996**, *100*, 16502−16513.

(91) Champagne, B. t.; Perpète, E. A.; van Gisbergen, S. J. A.; Baerends, E.-J.; Snijders, J. G.; Soubra-Ghaoui, C.; Robins, K. A.; Kirtman, B. Assessment of Conventional Density Functional Schemes for Computing the Polarizabilities and Hyperpolarizabilities of Conjugated Oligomers: An Ab Initio Investigation of Polyacetylene Chains. *J. Chem. Phys.* **1998**, *109*, 10489−10498.

(92) Halls, M. D.; Schlegel, H. B. Comparison of the Performance of Local, Gradient-Corrected, and Hybrid Density Functional Models in Predicting Infrared Intensities. *J. Chem. Phys.* **1998**, *109*, 10587−10593.

(93) Puzzarini, C.; Biczysko, M.; Barone, V. Accurate Harmonic/Anharmonic Vibrational Frequencies for Open-Shell Systems: Performances of the B3LYP/N07D Model for Semirigid Free Radicals Benchmarked by CCSD(T) Computations. *J. Chem. Theory Comput.* **2010**, *6*, 828−838.

(94) Koch, W.; Holthausen, M. C. *A Chemist's Guide to Density Functional Theory*; Wiley-VCH: New York, 2000.

(95) Biczysko, M.; Panek, P.; Scalmani, G.; Bloino, J.; Barone, V. Harmonic and Anharmonic Vibrational Frequency Calculations with the Double-Hybrid B2PLYP Method: Analytic Second Derivatives and Benchmark Studies. *J. Chem. Theory Comput.* **2010**, *6*, 2115−2125.

DOI: 10.1021/acs.jpcb.5b09769
J. Phys. Chem. B XXXX, XXX, XXX−XXX